

Supporting Information

Zn Doped FeCo LDH Nanoneedle Arrays with Partial Amorphous Phase for Efficient Oxygen Evolution Reaction

Jianxin Han^a, Jing Zhang^a, Tingting Wang^a, Qi Xiong^a, Wei Wang^{a,b}, Lixin Cao^{a,}, and Bohua Dong^{a,*}*

^a School of Materials Science and Engineering, Ocean University of China, 238

Songling Road, Qingdao, 266100 P. R. China

^b Aramco Research Center-Boston, Aramco Services Company, Cambridge, MA 02139, USA

*Corresponding author:

E-mail: dongbohua@ouc.edu.cn; caolixin@ouc.edu.cn

Number of pages: 24

Number of figures: 20

Number of schemes: 0

Number of tables: 2

Table of Contents

Figure S1 to Figure S20	Page S2 to Page S21
Table S1 to Table S2	Page S22 to Page S23
References	Page S24

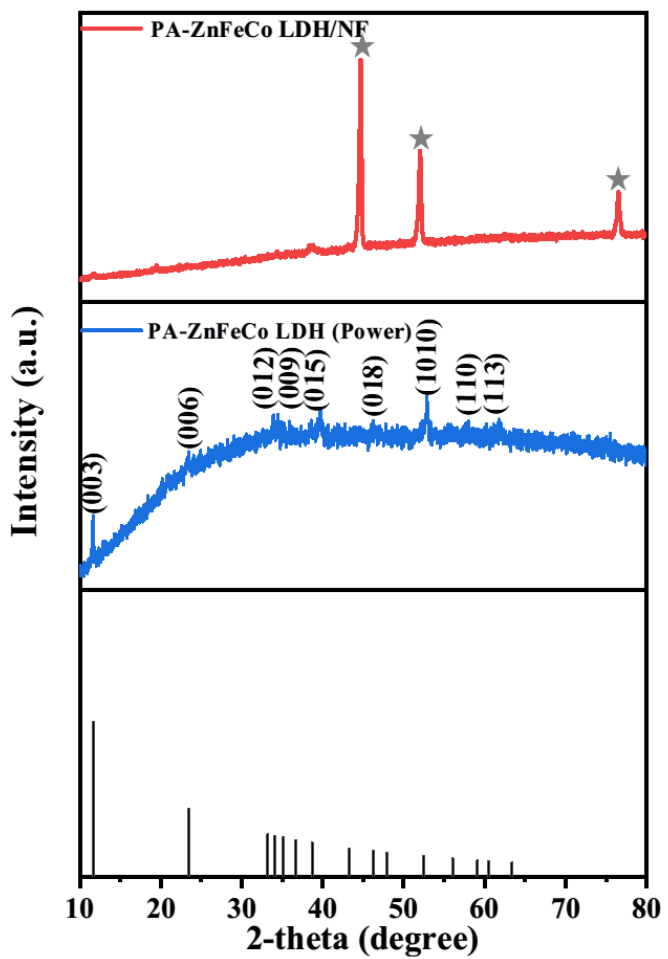


Figure S1 XRD patterns of the PA-ZnFeCo LDH/NF, the PA-ZnFeCo LDH (Power) and FeCo LDH (PDF#50-0235).

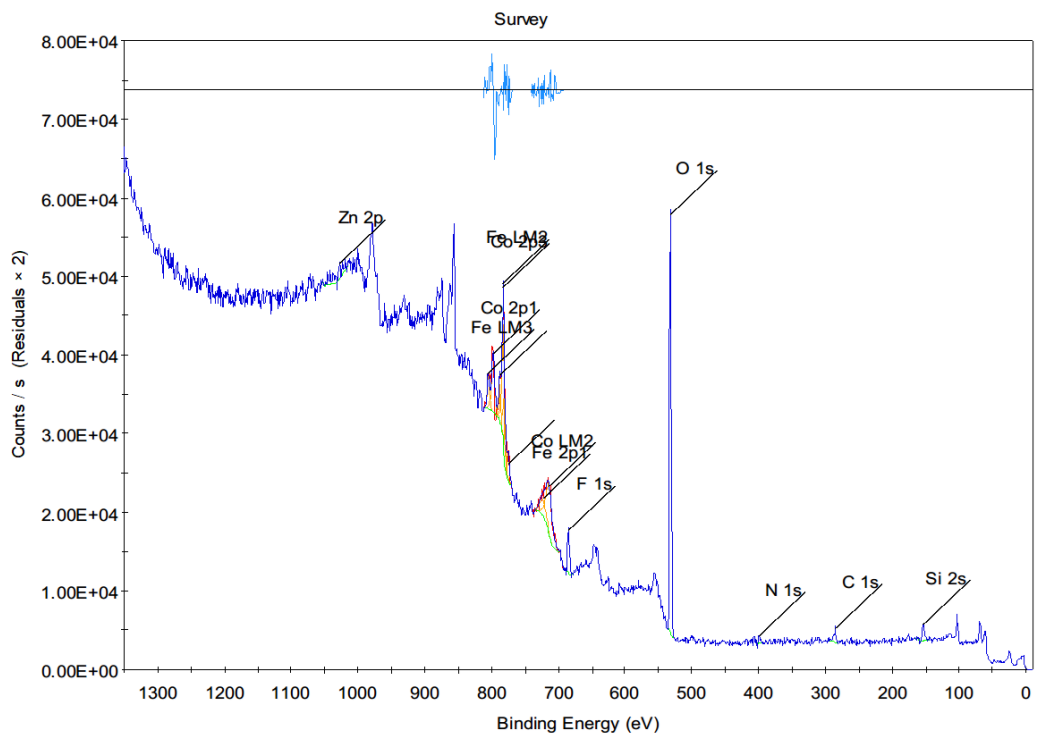


Figure S2 XPS survey of the PA-ZnFeCo LDH.

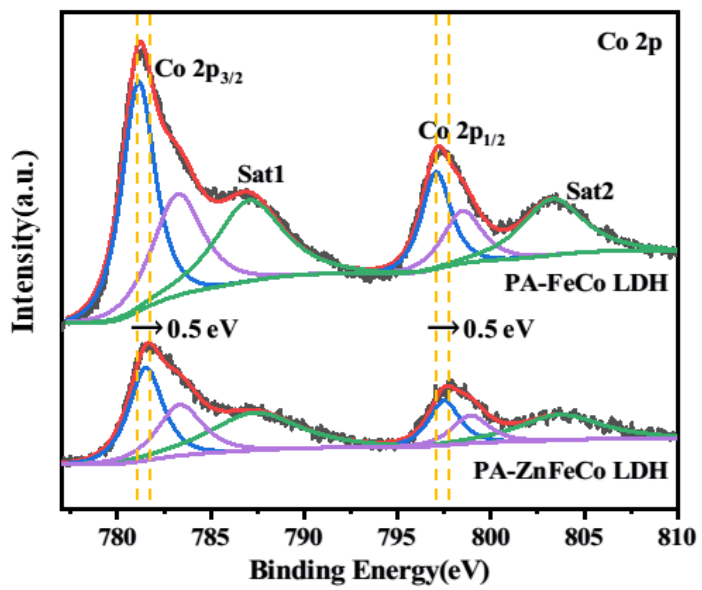


Figure S3 XPS spectra for the PA-FeCo LDH and PA-ZnFeCo LDH of Co 2p.

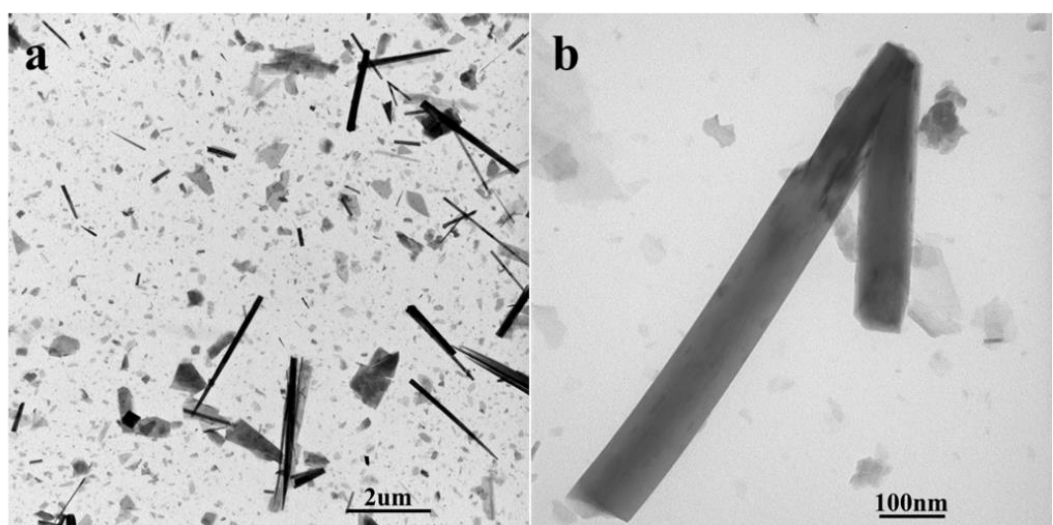


Figure S4 TEM images of the PA-ZnFeCo LDH.

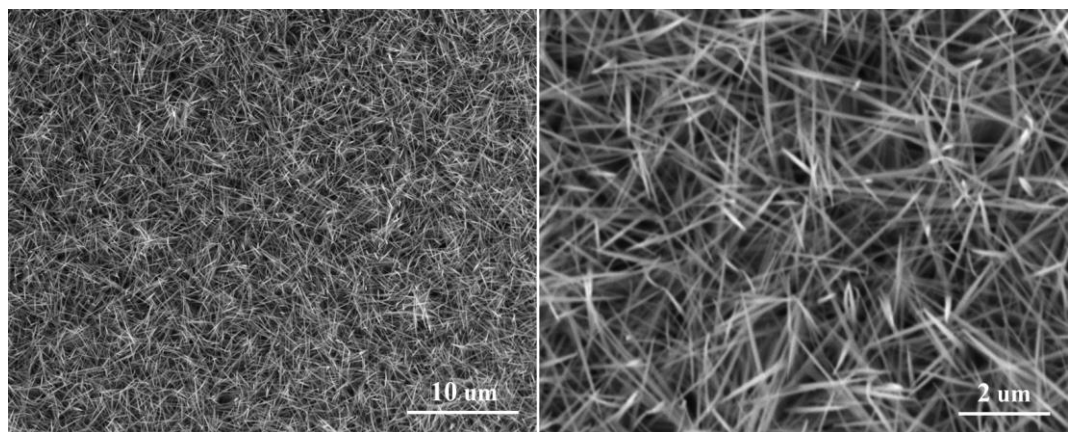


Figure S5 SEM images of the PA-FeCo LDH.

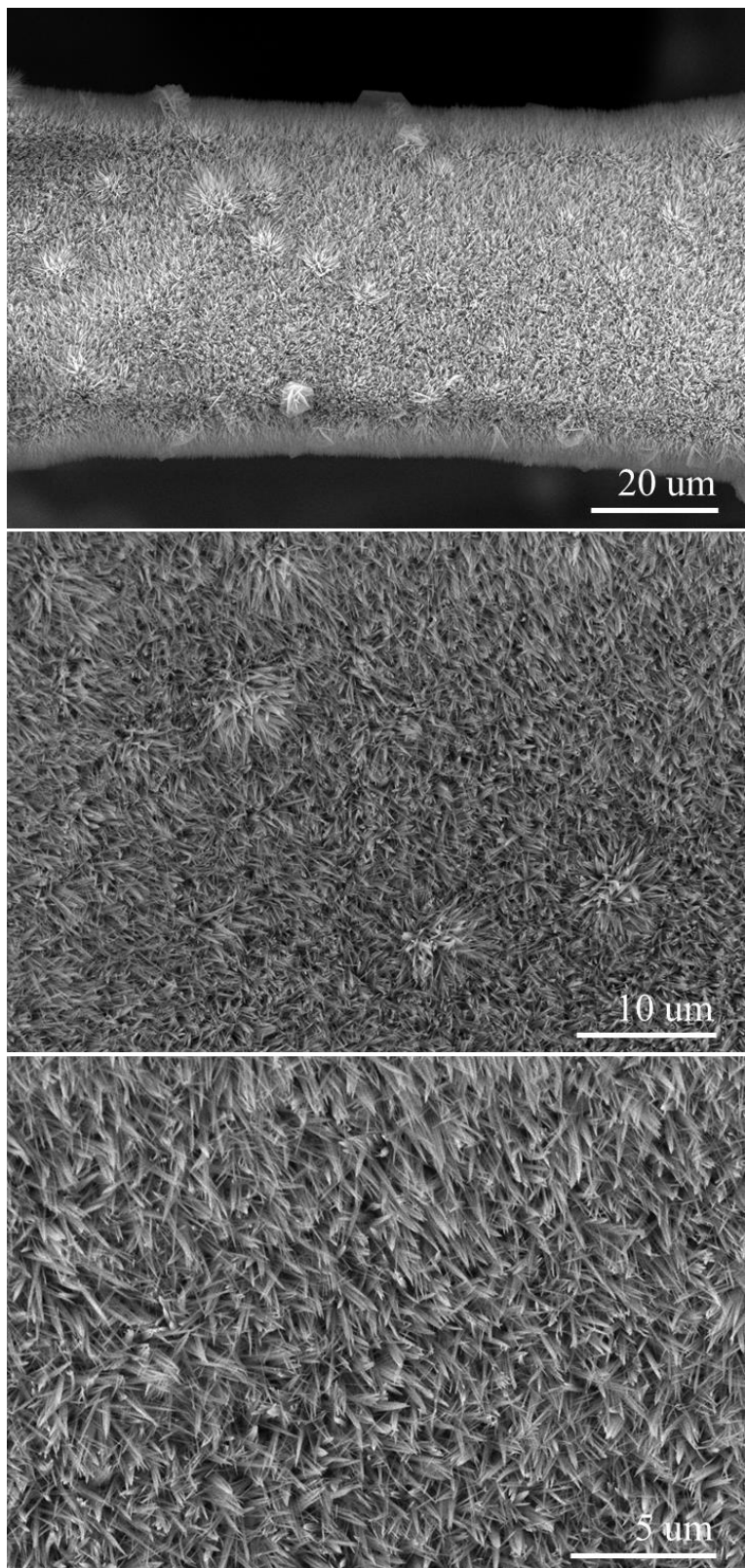


Figure S6 SEM images of the PA-ZnFeCo LDH with different magnification.

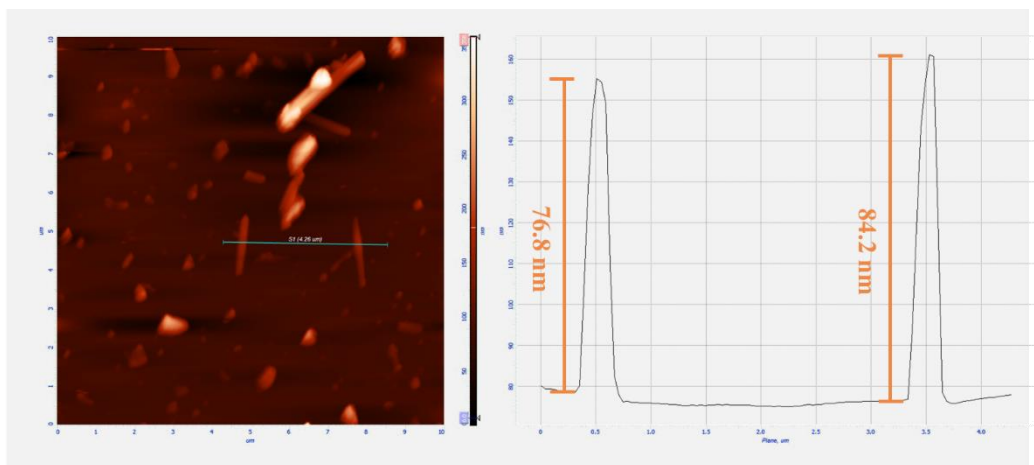


Figure S7 AFM images of the PA-ZnFeCo LDH.

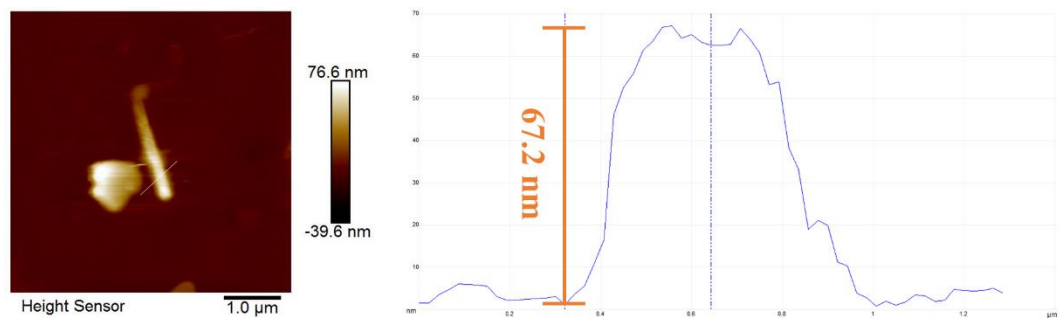


Figure S8 AFM images of the PA-FeCo LDH.

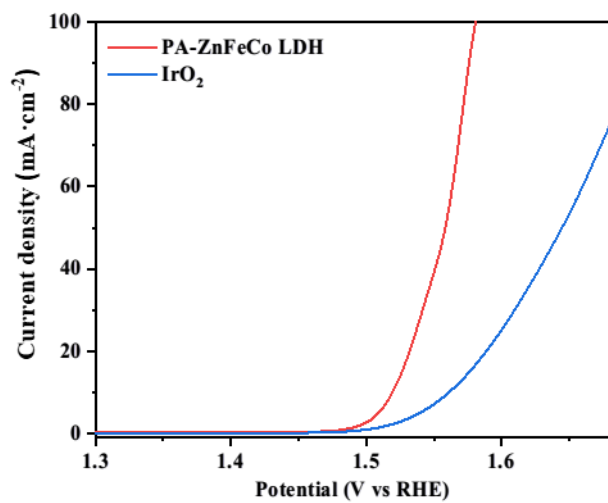


Figure S9 OER polarization curves of PA-ZnFeCo LDH (in powder form) and IrO₂ on glassy carbon substrate with a three-electrodes configuration in 1 M KOH electrolyte with 90% internal resistance (iR) compensation.

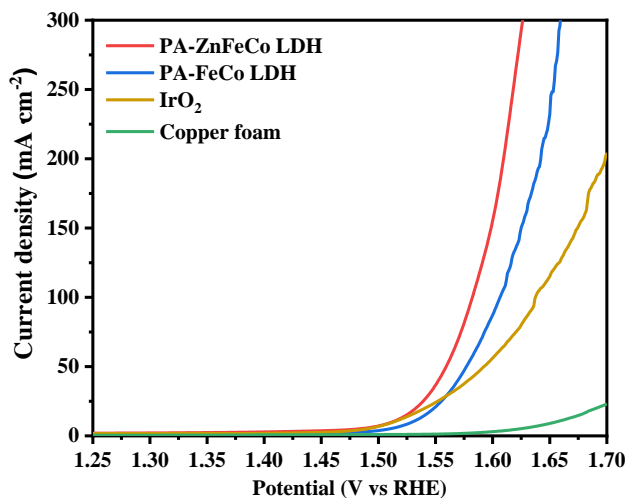


Figure S10 OER polarization curves of PA-ZnFeCo LDH/CF, PA-FeCo LDH/CF, IrO₂ and copper foam (CF) with a three-electrodes configuration in 1 M KOH electrolyte with 90% internal resistance (iR) compensation.

For a more comprehensive study of electrocatalytic performance of PA-ZnFeCo LDH, we have used copper foam (CF) as substrates, and the methods of synthesis and electrochemical characterization are the same as that of NF. As shown in Figure S9, the PA-ZnFeCo LDH/CF only requires overpotential of 282 and 352 mV to afford 10 mA cm⁻² (η_{10}) and 100 mA cm⁻² (η_{100}), respectively. They are much lower than PA-FeCo LDH/CF ($\eta_{10}=300$ mV; $\eta_{100}=376$ mV), IrO₂/CF ($\eta_{10}=283$ mV; $\eta_{100}=408$ mV), and bare copper foam ($\eta_{10}=425$ mV; $\eta_{100}=571$ mV), indicating a superior OER activity of the PA-ZnFeCo LDH/CF, which is consistent with Figure 4a.

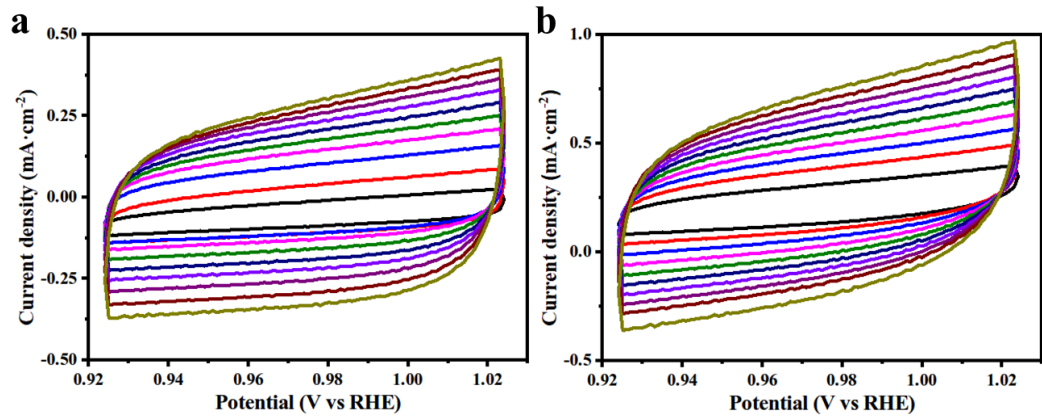


Figure S11 Cyclic voltammograms of (a) the PA-FeCo LDH; and (b) the PA-ZnFeCo LDH.

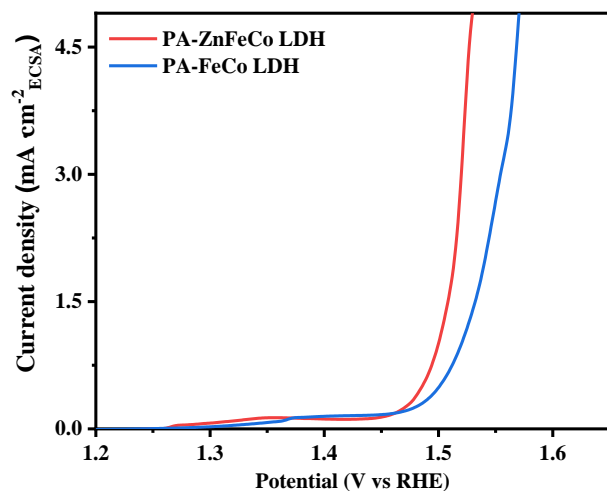


Figure S12 Normalized OER LSV curves of PA-ZnFeCo LDH/NF and PA-FeCo LDH/NF by ECSAs.

The electrochemical active surface area (ECSA) is evaluated by the electrochemical double-layered capacitance (C_{dl}) of samples according to the following equation:

$$ECSA = C_{dl}/C_s \quad (S1)$$

where C_s is the specific capacitance value of an ideal flat surface with 1 cm^{-2} of a real surface area. The general value of C_s is $60\text{ }\mu\text{F cm}^{-2}$.

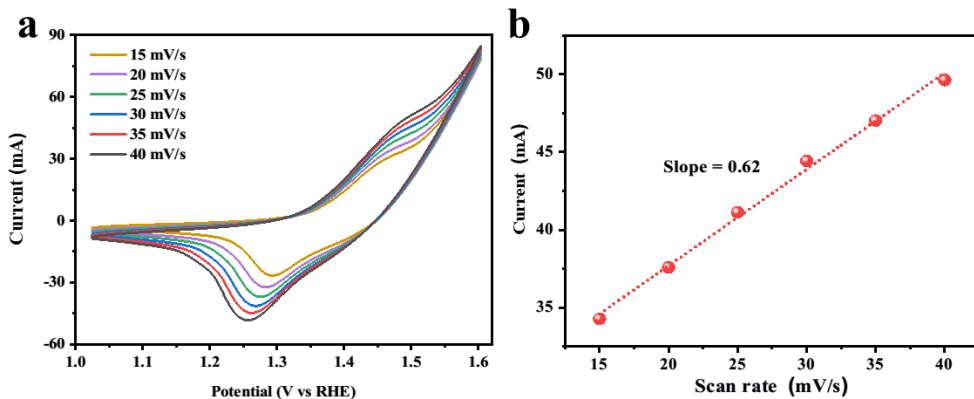


Figure S13 (a) CV of PA-ZnFeCo LDH/NF at different scan rates of 15, 20, 25, 30, 35 and 40 mV s⁻¹ in 1 M KOH. (b) Linear relationship of the oxidation peak currents vs. scan rate in the CV of (a).

In order to further explain the intrinsic activity of PA-ZnFeCo LDH/NF, the turnover frequency (TOF) at a certain overpotential was calculated according to the formula:

$$\text{TOF} = \frac{j \times A}{4 \times F \times m} \quad (\text{S2})$$

where j is current density at a certain overpotential (A cm^{-2}), A is surface area of the working electrode (1 cm^{-2}), F is Faraday constant ($96,485 \text{ C mol}^{-1}$) and m is concentration of active sites in the catalysts (mol cm^{-2}). m for oxygen evolution reaction (OER) could be determined by CV measurements at different scan rates in the voltage range where redox reaction occurs. A linear relationship exists between the scan rates and the current of the peak:

$$\text{Slope} = \frac{n^2 \times F^2 \times A \times m}{4 \times R \times T} \quad (\text{S3})$$

where n is the number of electrons transferred (here $n=1$), R is ideal gas constant, and T is absolute temperature.

The TOF values for PA-ZnFeCo LDH/NF are 0.29 and 1.47 s⁻¹ respectively, at an overpotential of 270 and 300 mV.

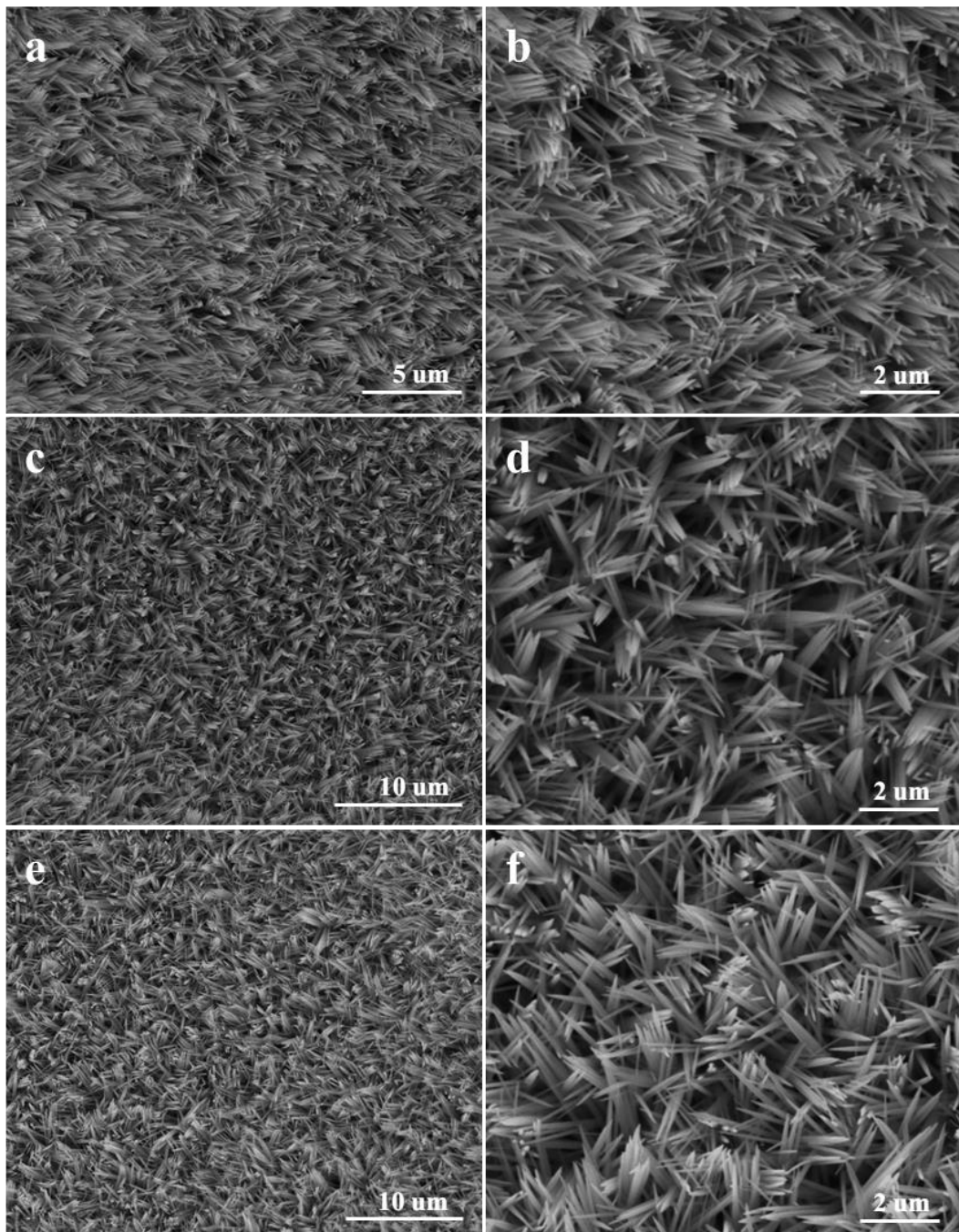


Figure S14 SEM images of the PA-ZnFeCo LDH with different ratio of Zn: Co. (a-b) the ratio of Zn: Co=1:4, (c-d) the ratio of Zn: Co=1:6, (e-f) the ratio of Zn: Co=1:10.

SEM images of the PA-ZnFeCo LDH with ratio of Zn: Co=1:8 was shown in Figure S6. All of the PA-ZnFeCo LDH nanoneedles with different ratio of Zn: Co are uniformly oriented on Ni foam. Moreover, these long nanoneedles grow vertically on the Ni foam support, with thin tips weaving in multiple directions.

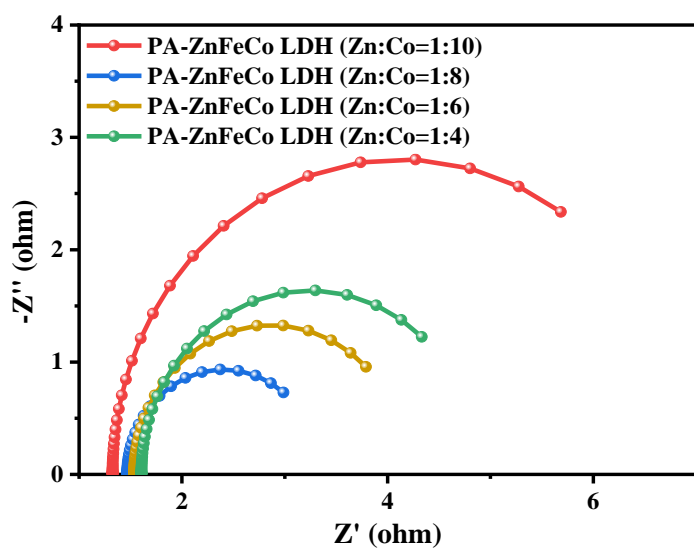


Figure S15 Nyquist plots of different electrodes at potential of 450 mV.

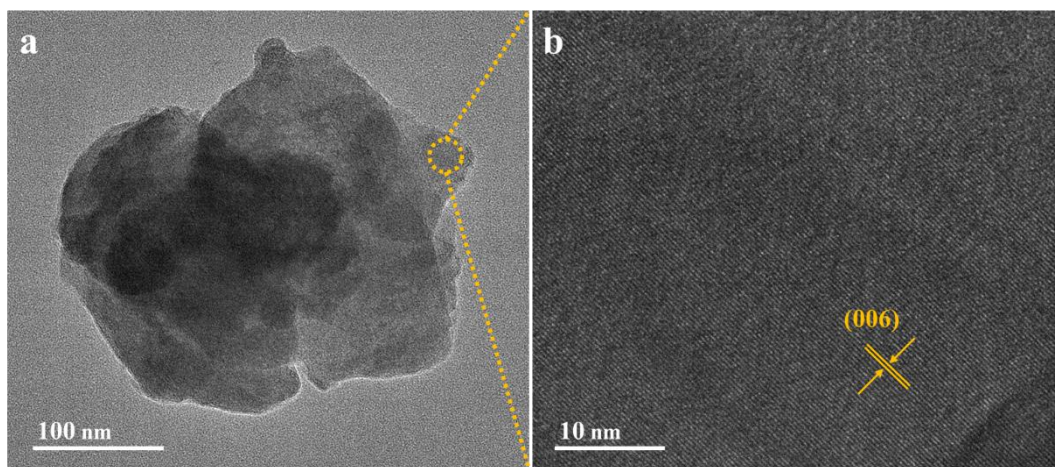


Figure S16 (a) TEM of the C-ZnFeCo LDH catalysts. (b) HRTEM of the range dotted circle in (a).

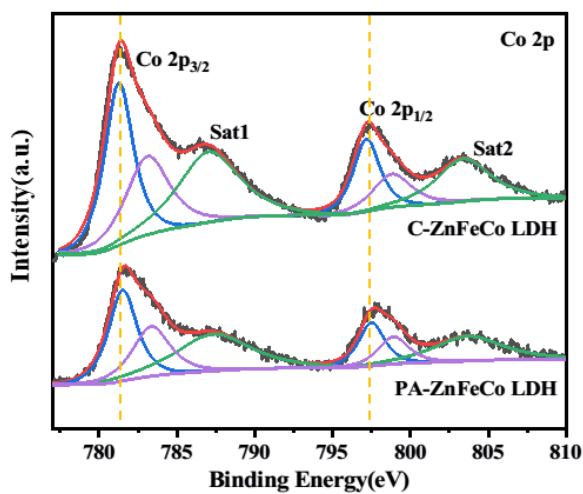


Figure S17 XPS spectra for the C-ZnFeCo LDH and PA-ZnFeCo LDH catalysts of Co 2p.

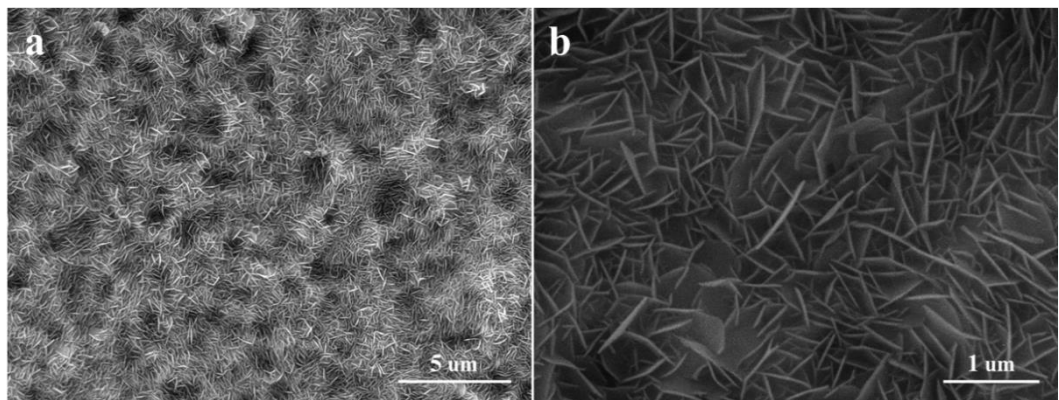


Figure S18 SEM images of the C-ZnFeCo LDH nanosheet arrays/NF.

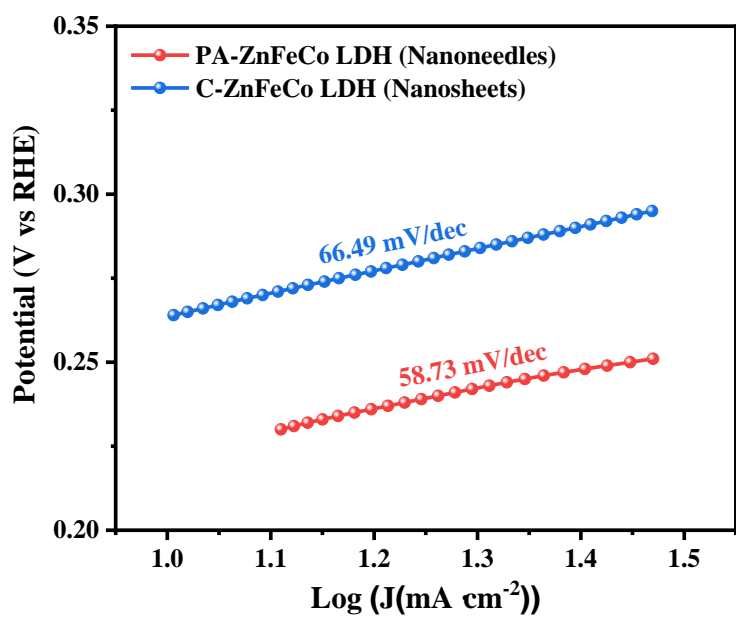


Figure S19 Tafel plots of the C-ZnFeCo LDH (Nanosheets) catalyst and the PA-ZnFeCo LDH (Nanoneedles) catalyst.

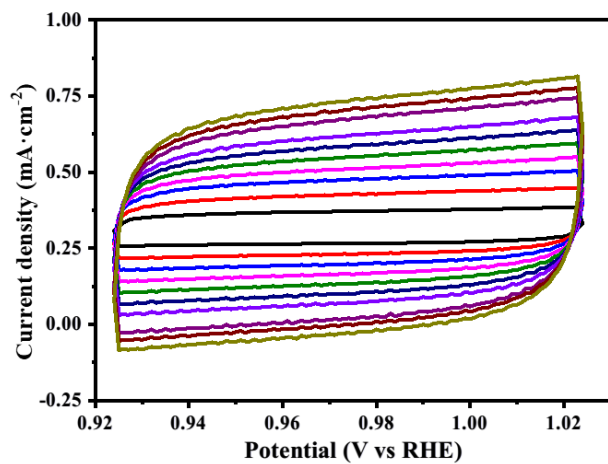


Figure S20 Cyclic voltammograms of the C-ZnFeCo LDH catalyst.

Table S1 ICP-OES characterization of the PA-ZnFeCo LDH samples.

Sample	Element	CC (mg kg ⁻¹)	Sample	Element	CC (mg kg ⁻¹)	
PA-ZnFeCo LDH-1	Zn	42197	PA-ZnFeCo LDH-2	Zn	42273	
	Fe	102273		Fe	103030	
	Co	246212		Co	246970	
Theoretical atomic ratio of Zn:Fe:Co = 1:3:8						
Experimental atomic ratio of Zn:Fe:Co = 1:2.85:6.48						

Table S2 Comparison of the state-of-the-art LDH electrocatalysts for OER in alkaline medium (j: current density; η: overpotential)

Electrocatalyst	Substrate	Electrolyte	j (mA cm ⁻²)	η (mV)	Tafel Slope (mV dec ⁻¹)	Reference
PA-ZnFeCo LDH	Ni foam	1M KOH	10 100	221 276	58.73	This work
NiFe LDHs	Glassy carbon	1M KOH	10	~350	64	1
NiV LDHs	Glassy carbon	1M KOH	10	~310	50	1
NiFe LDH	Ni foam	1M KOH	10 100	240 460	-	2
CoFe LDH	Indium-tin oxide	1M KOH	10	400	83	3
	Ni foam	1M KOH	10 100	300 420	-	3
NiCo LDH	Carbon paper	1M KOH	10	367	40	4
ZnCo LDH	Glassy carbon	0.1M KOH	2	375	101	5
CoMn LDH	Glassy carbon	1M KOH	10	324	43	6
(Co,Ni)Se ₂ @NiFe LDH	Glassy carbon	1M KOH	10	277	75	7
Calixarene intercalated NiCo LDH	Carbon nano-onion	1M KOH	10	290	31	8
Mo- and Fe-modified Ni(OH) ₂ /NiOOH	Ni foam	1M KOH	100	280	75	9
NiFeCr LDH	Ni foam	1M KOH	100	255	29	10

References

- (1) Fan, K.; Chen, H.; Ji, Y.; Huang, H.; Claesson, P. M.; Daniel, Q.; Philippe, B.; Rensmo, H.; Li, F.; Luo, Y. and Sun, L. Nickel-vanadium monolayer double hydroxide for efficient electrochemical water oxidation. *Nat. Commun.* **2016**, *7*, 11981, DOI 10.1038/ncomms11981.
- (2) Luo, J.; Im, J.-H.; Mayer, M. T.; Schreier, M.; Nazeeruddin, M. K.; Park, N.-G.; Tilley, S. D.; Fan, H. J. and Graetzel, M. Water photolysis at 12.3% efficiency via perovskite photovoltaics and Earth-abundant catalysts. *Science* **2014**, *345* (6204) 1593-1596, DOI 10.1126/science.1258307.
- (3) Feng, L.; Li, A.; Li, Y.; Liu, J.; Wang, L.; Huang, L.; Wang, Y. and Ge, X. A Highly Active CoFe Layered Double Hydroxide for Water Splitting. *Chempluschem* **2017**, *82* (3) 483-488, DOI 10.1002/cplu.201700005.
- (4) Liang, H.; Meng, F.; Caban-Acevedo, M.; Li, L.; Forticaux, A.; Xiu, L.; Wang, Z. and Jin, S. Hydrothermal Continuous Flow Synthesis and Exfoliation of NiCo Layered Double Hydroxide Nanosheets for Enhanced Oxygen Evolution Catalysis. *Nano Lett.* **2015**, *15* (2) 1421-1427, DOI 10.1021/nl504872s.
- (5) Qiao, C.; Zhang, Y.; Zhu, Y.; Cao, C.; Bao, X. and Xu, J. One-step synthesis of zinc-cobalt layered double hydroxide (Zn-Co-LDH) nanosheets for high-efficiency oxygen evolution reaction. *J. Mater. Chem. A* **2015**, *3* (13) 6878-6883, DOI 10.1039/c4ta06634k.
- (6) Song, F. and Hu, X. Ultrathin Cobalt-Manganese Layered Double Hydroxide Is an Efficient Oxygen Evolution Catalyst. *J. Am. Chem. Soc.* **2014**, *136* (47) 16481-16484, DOI 10.1021/ja5096733.
- (7) Li, J.-G.; Sun, H.; Lv, L.; Li, Z.; Ao, X.; Xu, C.; Li, Y. and Wang, C. Metal-Organic Framework-Derived Hierarchical (Co,Ni)Se-2@NiFe LDH Hollow Nanocages for Enhanced Oxygen Evolution. *ACS Appl. Mater. Interfaces* **2019**, *11* (8) 8106-8114, DOI 10.1021/acsami.8b22133.
- (8) Waghmode, B. J.; Gaikwad, A. P.; Rode, C. V.; Sathaye, S. D.; Patil, K. R. and Malkhede, D. D. Calixarene Intercalated NiCo Layered Double Hydroxide for Enhanced Oxygen Evolution Catalysis. *ACS Sustainable Chem. Eng.* **2018**, *6* (8) 9649-9660, DOI 10.1021/acssuschemeng.7b04788.
- (9) Jin, Y.; Huang, S.; Yue, X.; Du, H. and Shen, P. K. Mo- and Fe-Modified Ni(OH)(2)/NiOOH Nanosheets as Highly Active and Stable Electrocatalysts for Oxygen Evolution Reaction. *ACS Catal.* **2018**, *8* (3) 2359-2363, DOI 10.1021/acscatal.7b04226.
- (10) Bo, X.; Li, Y.; Hocking, R. K. and Zhao, C. NiFeCr Hydroxide Holey Nanosheet as Advanced Electrocatalyst for Water Oxidation. *ACS Appl. Mater. Interfaces* **2017**, *9* (47) 41239-41245, DOI 10.1021/acsami.7b12629.